Emergence of Homochirality in Chemical Systems

Department of Applied Chemistry
Faculty of Science & Technology

Keio University

Kouichi Asakura

Keio

http://www.keio.ac.jp/

Year 2008

KEIO 150
Design the Future

History

Keio History & World Timeline

1858 Yukichi Fukuzawa establishes a school for Dutch studies in Edo (now Tokyo).

1861 The Civil War breaks out in the United States.

1863 Fukuzawa's school switches its focus to English studies.

1868 Fukuzawa's school moves to a new location and is renamed after the Keio Era. Three years later, the Keio school moves to Mita, the current site of Keio University's main campus.

1868 The Meiji Restoration begins in Japan.

1869 The Suez Canal opens, shortening the sea route between Europe and Asia.

1874 Keio Yochisha Elementary School is established.

1890 Keio University establishes a college with Departments of Law, Literature (presently Faculty of Letters), and Economics.

1898 Keio becomes a comprehensive educational institution with college, secondary and elementary schools.

1944 The Fujiwara Institute of Technology is donated to Keio University, and becomes the Faculty of Engineering.

1945 World War Two comes to an end.

Biorhythms

Temporary Periodic Patterns

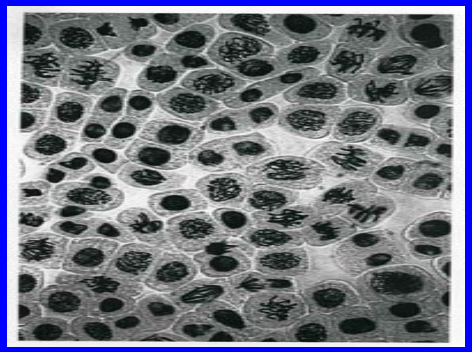

Cell cycle
Circadian rhythm
Pulsation

Spatially Periodic Patterns

Surface of Animal Body

Once you know the concept of Dissipative Structure
Temporary and Spatially Periodic Patterns can be realized by Artificial Chemical Reaction !!

QuickTimeý Ç² YUV420 ÉRÁÍÉíÉbÉN ôLíÉÉvÉçÉOÉäÉÁ Ç™Ç±ÇÄÉsÉNÉ´ÉÉÇ¼á©ÇÈÇŽÇ½Ç…ÇÓíKóvÇ-Ç ÃB

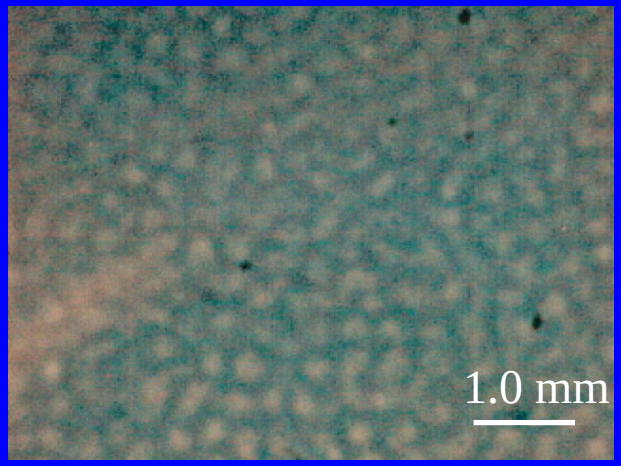

Bray Reaction: W. C. Bray, *J. Am. Chem. Soc.*, **1921**, *43*, 1262.
Belouzov-Zhabotisky Reaction: B. P. Belouzov, **1958**.
Brusselator: I. Prigogine, R. Lefever, *J. Phys. Chem.*, **1958**, *48*, 1965.

Modeling: A. M. Turing, *Philos. Trans. Roy. Soc. London*, **1952**, *B 237*, 37.
Experimental realization: V. Castets, E. Dulos, J. Boissonade, P. De Kepper, *Phys. Rev. Lett.*, **1990**, *64*, 2953.

Self-Organizationin Nonequilibrium System : Dissipative Structure

Proposed by Ilya Prigogine: Nobel Laureate in Chemistry in 1977

Energy
or
Higher Chemical Potential Matter

Irreversible Dissipative Processes

- **Reaction**
- **Diffusion**
- **Heat Conduction**

Growth of Fluctuation

Self-Organized State (Dissipative Structure)

- **Oscillation**
- **Pattern Formation**
- **Chiral Symmetry Breaking**

$$\frac{d_i S}{dt} > 0$$

Lower Chemical Potential Matter

Chemical Oscillation

Belouzov-Zhbotinsky Reaction (1958)

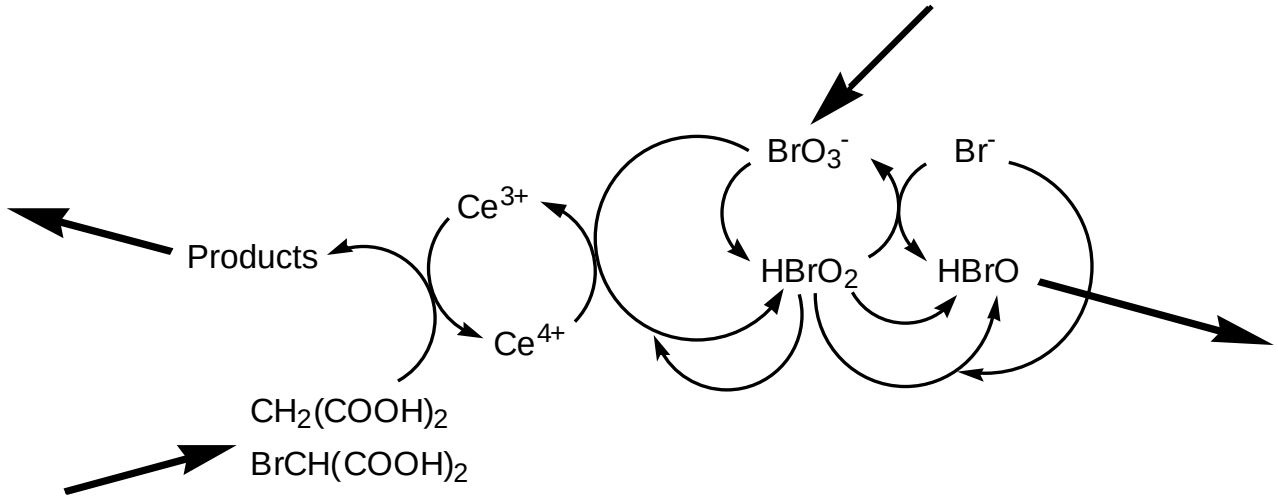

Brusselator (1968)

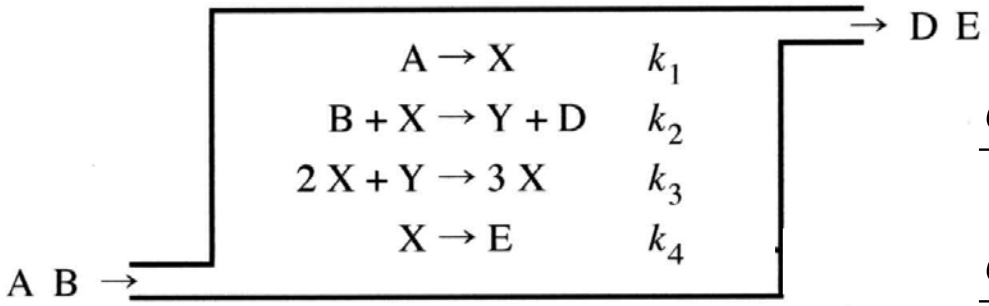

$$\frac{dX}{dt} = k_1 A - k_2 BX + k_3 X^2 Y - k_4 X$$

$$\frac{dY}{dt} = k_2 BX - k_3 X^2 Y$$

Spatial Pattern Formation

Turing Model (1942)

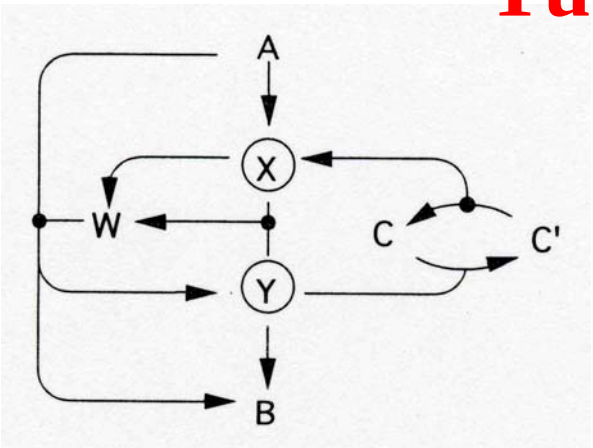

$$\frac{\partial X}{\partial t} = -7X^2 - 50XY + 57 + D_X \frac{\partial^2 X}{\partial l^2}$$

$$\frac{\partial Y}{\partial t} = 7X^2 + 50XY - 2Y - 55 + D_Y \frac{\partial^2 Y}{\partial l^2}$$

Turing Pattern Fomation by CIMA Reaction (1990)

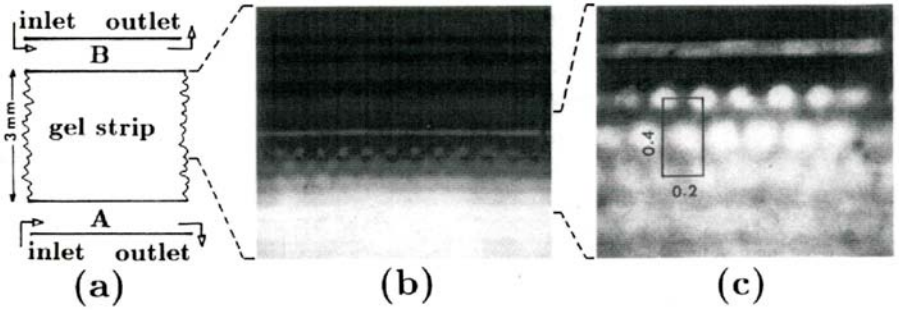

FIG. 1. Sustained chemical pattern in the gel strip reactor. (a) Sketch of the reactor: The gel strip is tightly squeezed between two flat plates 1 mm apart. Reactants are fed through the well-mixed reservoirs *A* and *B*. (b) Contrast-enhanced image: Dark regions correspond to reduced states colored in blue; clear zones correspond to oxidized states. (c) Enlarged image of the region of pattern (dimensions in mm). Experimental conditions: The gel is prepared by dissolving in 100 ml of water: 17.1 g acrylamide, 0.10 g *N*,*N'*-methylene-bisacrylamide, 0.70 g ammonium persulfate, 1.0 g triethanolamine, and 2.8 g thiodène (iodine color indicator from PROLABO). A thin uniformly flat layer of the solution is left to polymerize at 0 °C for 1 h. The resulting sheet of polymer is then thoroughly washed and set to swell in water for 24 h before the reactor strip is cut off. After swelling of the gel, the concentration of the color indicator (taken as amylose) is $\sim 10^{-4}$ mole/l and does not significantly decay during the experiments. Boundary feed compositions: in *A*, $[NaClO_2]_0^A = 2.6\times10^{-2}$ mole/l, $[KI]_0^A = 3.0\times10^{-3}$ mole/l, $[NaOH]_0^A = 3\times10^{-3}$ mole/l, $[Na_2SO_4]_0^A = 3\times10^{-3}$ mole/l; in *B*, $[CH_2(COOH)_2]_0^B = 9\times10^{-3}$ mole/l, $[KI]_0^B = 3.0\times10^{-3}$ mole/l, $[H_2SO_4]_0^B = 10^{-2}$ mole/l, $[NaOH]_0^B = 3\times10^{-3}$ mole/l, $[Na_2SO_4]_0^B = 3\times10^{-3}$ mole/l. Temperature: 7 °C.

Linear Stability Analysis for Two Variables System

Rate equation (Time derivative of concentration)

$$\frac{dX}{dt} = f(X,Y)$$

$$\frac{dY}{dt} = g(X,Y)$$

Steady state solution

$$f(X,Y) = 0,\ g(X,Y) = 0 \longrightarrow X_{SS}, Y_{SS}$$

Perturbation by Fluctuation

$$X = X_{SS} + \delta X$$

$$Y = Y_{SS} + \delta Y$$

Linear Stability Analysis for Two Variables System

First order term of Taylor series

$$\frac{d\delta X}{dt} = \left(\frac{\partial f}{\partial X}\right)_{SS} \delta X + \left(\frac{\partial f}{\partial Y}\right)_{SS} \delta Y$$

$$\frac{d\delta Y}{dt} = \left(\frac{\partial g}{\partial X}\right)_{SS} \delta X + \left(\frac{\partial g}{\partial Y}\right)_{SS} \delta Y$$

Fluctuation

$$\delta X = c_1 \exp(\lambda t), \delta Y = c_2 \exp(\lambda t)$$

Jacobian matrix

$$\mathbf{J} = \begin{bmatrix} \frac{\partial f}{\partial X} & \frac{\partial f}{\partial Y} \\ \frac{\partial g}{\partial X} & \frac{\partial g}{\partial Y} \end{bmatrix}_{SS} \qquad \mathbf{C} = \begin{bmatrix} c_1 \\ c_2 \end{bmatrix} \qquad (\mathbf{J} - \lambda \mathbf{I})\mathbf{C} = \mathbf{0}$$

Linear Stability Analysis for Two Variables System

Characteristic equation

$$\lambda^2 - \lambda \mathrm{tr}(\mathbf{J}) + \det(\mathbf{J}) = 0$$

Stability of steady state

$$\mathrm{tr}(\mathbf{J}) < 0,\ \det(\mathbf{J}) > 0 \longrightarrow \boxed{\textbf{Stable}}$$

$$\updownarrow$$

Other conditions $\longrightarrow$ **Unstable**

Oscillating Mouse & Traveling Wave Mouse

"Traveling stripes on the skin of a mutant mouse"

N. Suzuki, M. Hirata, S. Kondo, *P. Natl. Acad. Sci. USA*, **100**, 9680-9685 (2003)

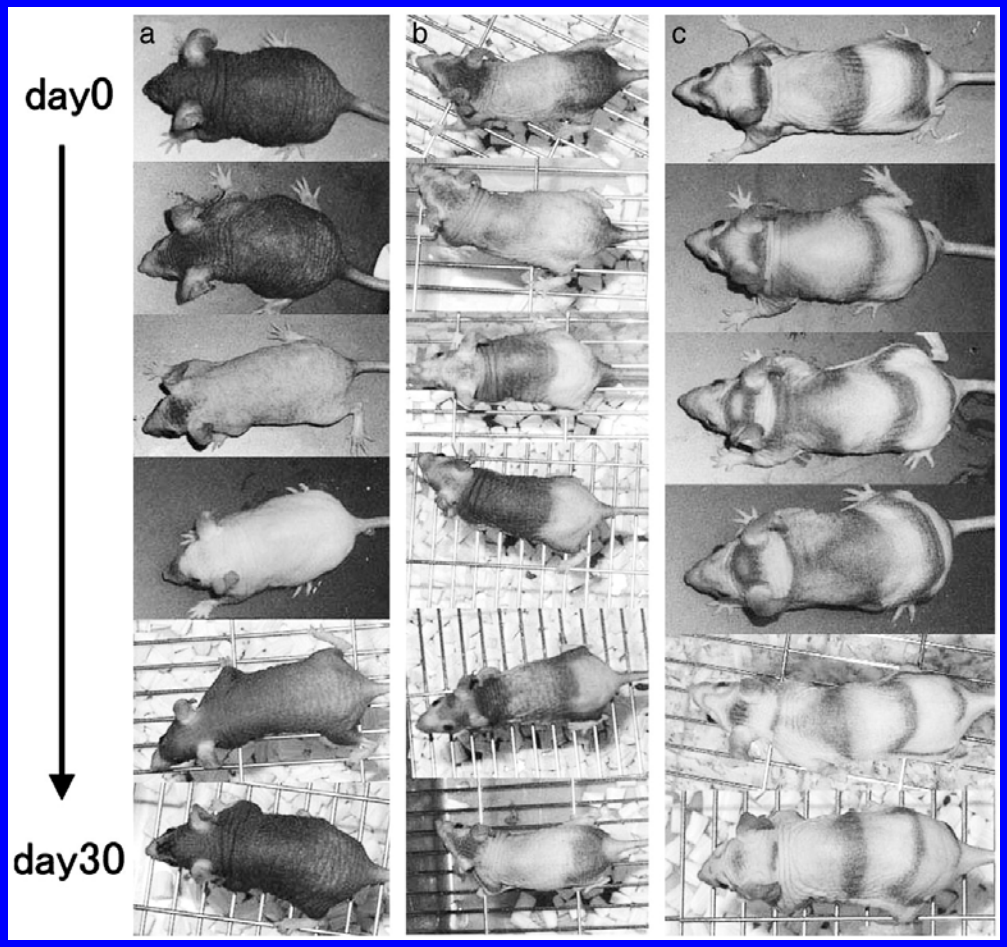

Fig. 3. Pattern change of a homozygous *Foxn1tw* mouse during the 30-day cycle. (*a*) Days 30-60. (*b*) Days 90-120. (*c*) Days 210-240 after birth. Pictures are taken at 5-day intervals with a Nikon digital camera. The pattern change shown here is typical for a homozygous *Foxn1tw* mouse.

Chiral Aymmetry

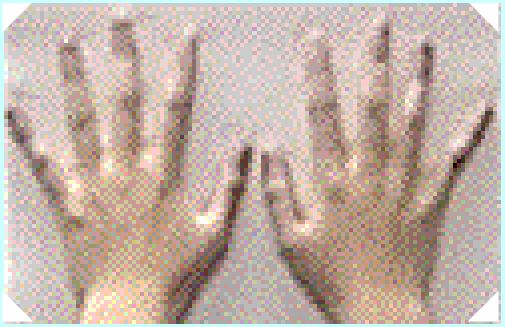

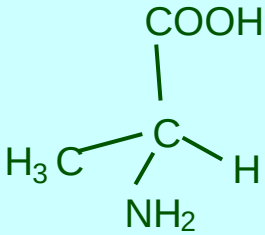

L-ƒAƒ‰ƒjƒ“

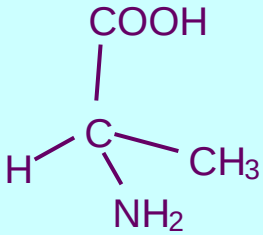

D-ƒAƒ‰ƒjƒ“

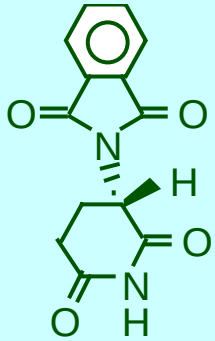

L-ƒTƒŠƒhƒ}ƒCƒh

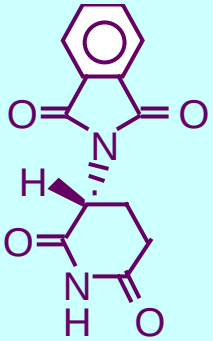

D-ƒTƒŠƒhƒ}ƒCƒh

α-Helix of Protein and Double Helix of DNA

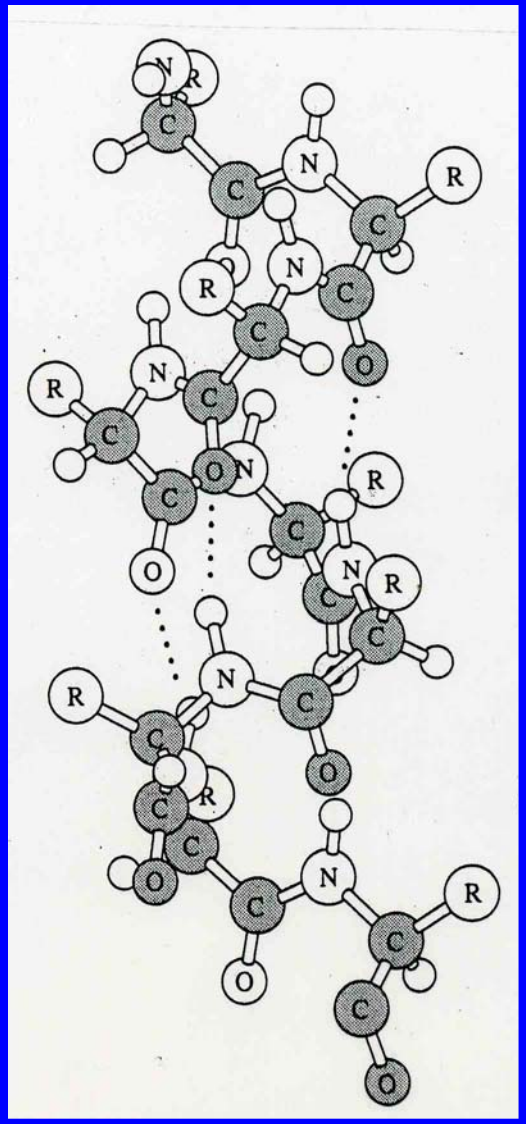

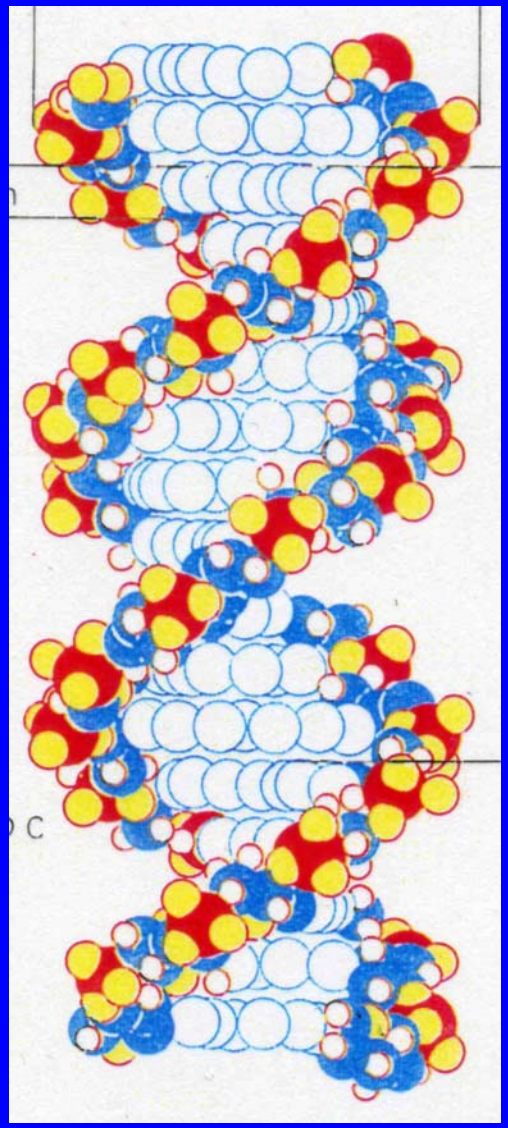

Frank's Model

$$\frac{dL}{dt} = k_1 A + k_2 AL - k_3 LD$$

$$\frac{dD}{dt} = k_1 A + k_2 AD - k_3 LD$$

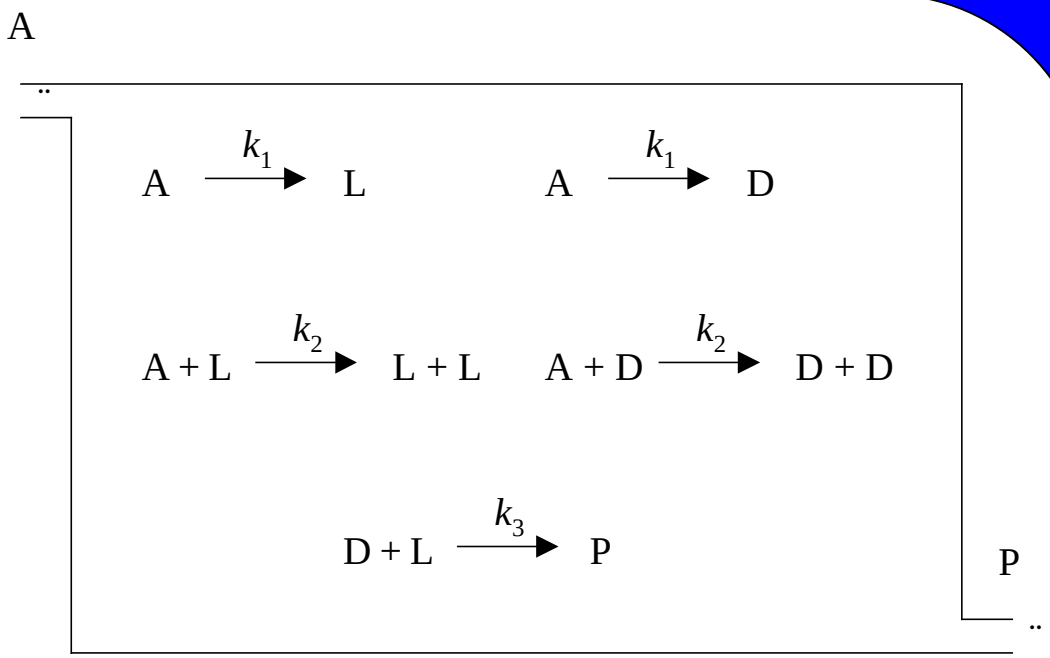

$$L = D = \frac{Ak_2 + \sqrt{(Ak_2)^2 + 4Ak_1k_3}}{2k_3}$$

$$J = \begin{bmatrix} Ak_2 - k_3 D & -k_3 L \\ -k_3 D & Ak_2 - k_3 L \end{bmatrix}$$

$$\lambda_1 = Ak_2 > 0$$

$$\lambda_2 = -\sqrt{(Ak_2)^2 + 4Ak_1k_3}$$

D. K. Kondepudi, G. W. Nelson, *Nature*, **1985**, *314*, 438-441.

Chiral Symmetry Breaking Transition by Kondepudi & Nelson's Model

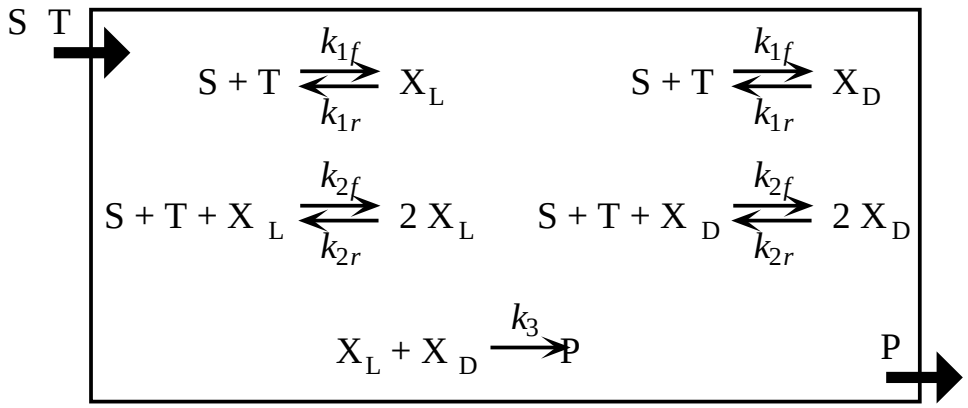

$$\lambda = [S][T]$$

$$\alpha = ([X_L] - [X_D]) / ([X_L] - [X_D])$$

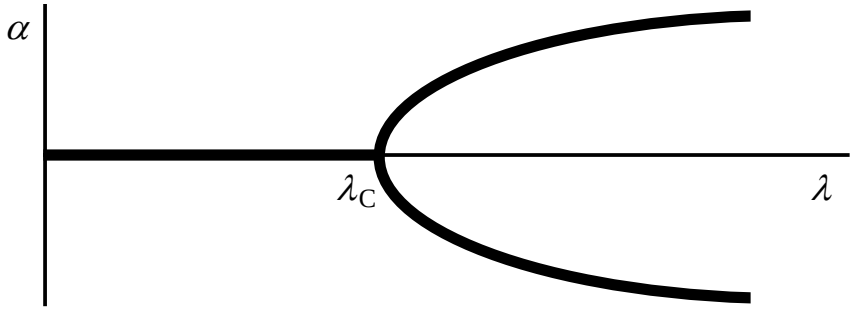

$$\frac{d\alpha}{dt} = -A\alpha^3 + B(\lambda - \lambda_C)\alpha$$

D. K. Kondepudi, G. W. Nelson, *Nature*, **1985**, *314*, 438-441.

Frank's Model

$$\frac{dL}{dt} = k_1 A + k_2 AL - k_3 LD$$

$$\frac{dD}{dt} = k_1 A + k_2 AD - k_3 LD$$

$$L_{SS} = D_{SS} = \frac{k_2 A + \sqrt{(k_2 A)^2 + 4 k_1 k_3 A}}{2 k_3}$$

$$J = \begin{bmatrix} k_2 A - k_3 D & -k_3 L \\ -k_3 D & k_2 A - k_3 L \end{bmatrix}_{SS}$$

$$\left.\begin{aligned} \lambda_1 &= k_2 A > 0 \\ \lambda_2 &= -\sqrt{(k_2 A)^2 + 4 k_1 k_3 A} < 0 \end{aligned}\right\} \longrightarrow \text{Saddle point}$$

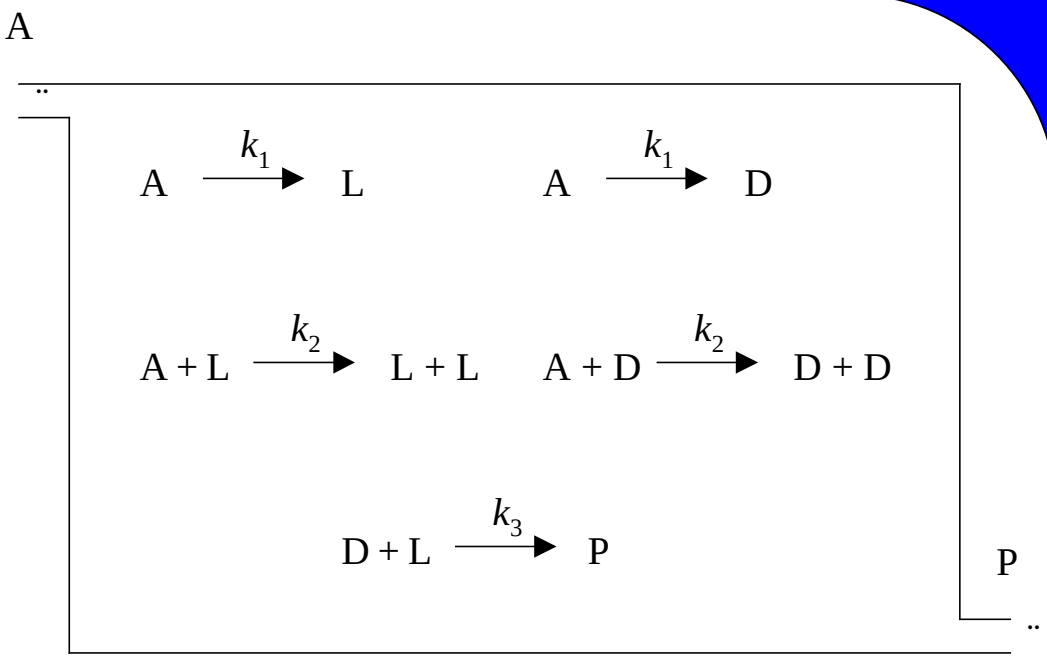

F. C. Frank, *Biophys. Acta*, **1953**, *11*, 459-463.

Convection Pattern Formation on Earth

Sun

Constraint

Energy: E

Earth

$E > E_C$

Response

Spontaneous Generation of Convection Patterns

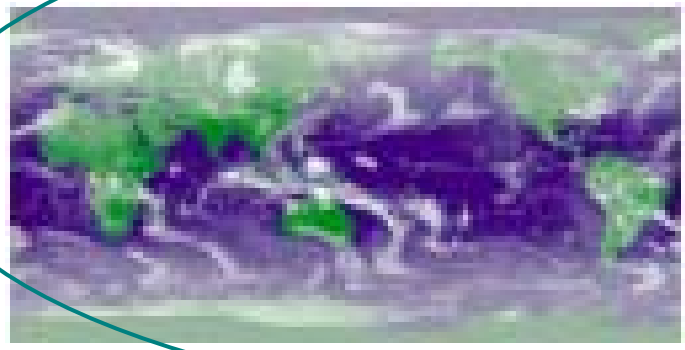

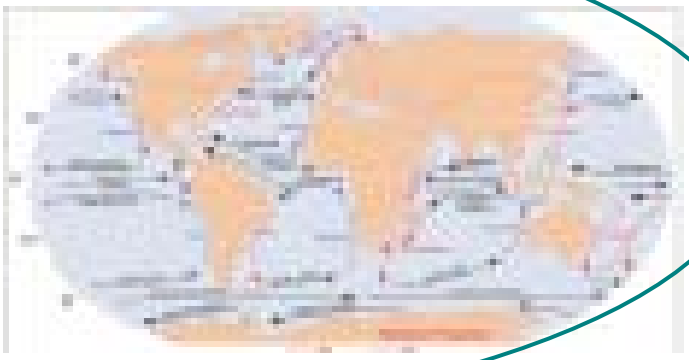

Chiral Symmetry Breaking Transition

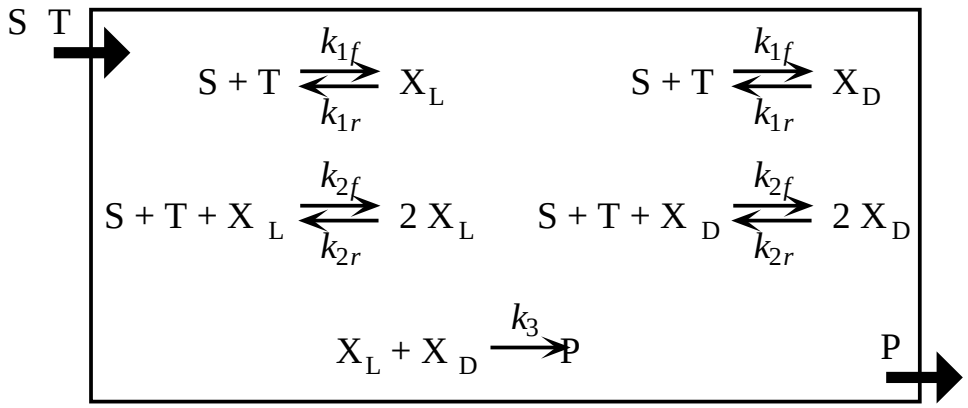

$$\lambda = [S][T]$$

$$\alpha = ([X_L] - [X_D]) / ([X_L] - [X_D])$$

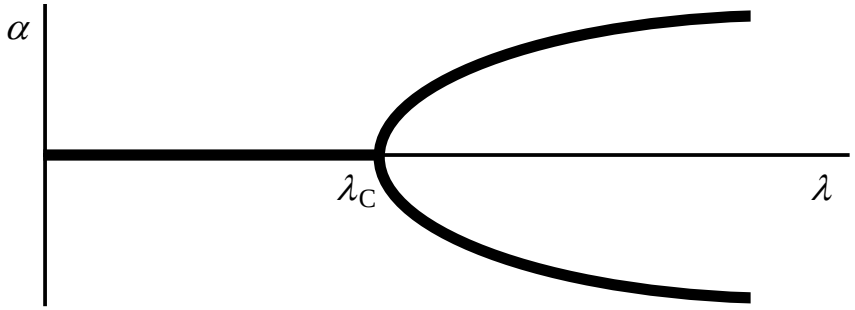

$$\frac{d\alpha}{dt} = -A\alpha^3 + B(\lambda - \lambda_C)\alpha$$

D. K. Kondepudi, G. W. Nelson, *Nature*, **1985**, *314*, 438-441.

Chiral Autocatalysis in Crystallization of 1, 1'-Binaphthyl

1, 1'-Binaphthyl m.p.: Racemic crystal: 145°C; Chial crystal: 158°C

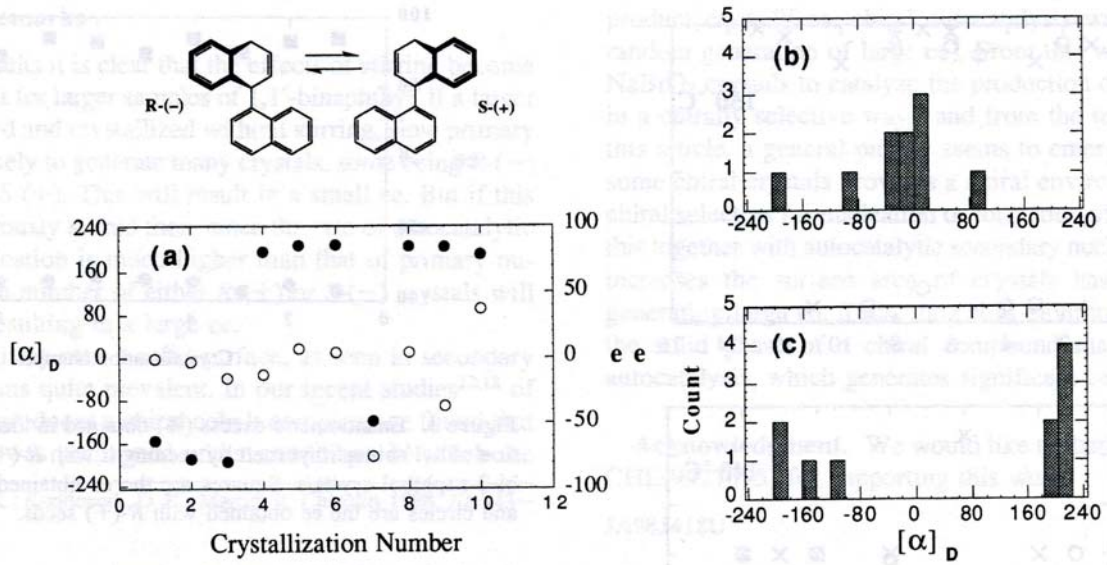

Figure 1. Specific rotation $[\alpha]_D$ and enantiomeric excess (ee), obtained in crystallizations of 2.00 g samples of binaphthyl melt at 150 °C. The crystals were dissolved in benzene and the optical rotation of the solution was measured. (a) The specific rotation of 10 stirred (filled circles) and 10 unstirred crystallizations (open circles) of binaphthyl. 100% optical purity corresponds to $[\alpha]_D$ 245°. (b) Histogram of $[\alpha]_D$ for unstirred samples. (c) Histograms of $[\alpha]_D$ for the stirred samples.

D. K. Kondepudi, K. Asakura, *et al.*, *J. Am. Chem. Soc.*, **1999**, *121*, 1448-1451.

Crystal Growth of of 1, 1’-Binaphthyl

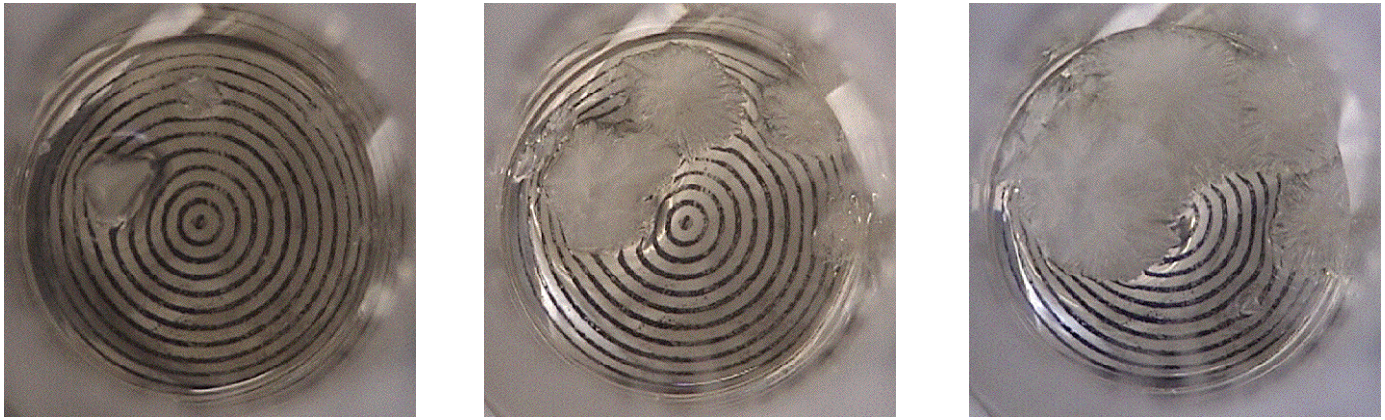

K. Asakura, D. K. Kondepudi, *et al.*, *Chirality*, **2002**, *14*, 85-89.

Crystal Growth Front as an Open System

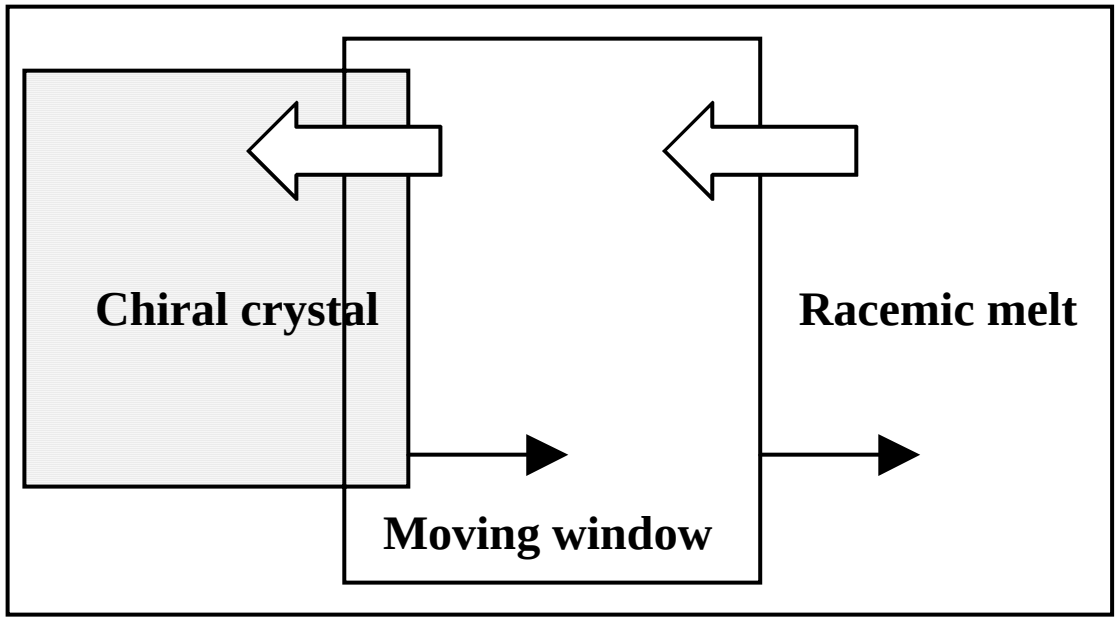

K. Asakura, D. K. Kondepudi, *et al.*, *Chirality*, **2004**, *16*, 131-136.

Chiral Symmetry Breaking Transition in Crystallization of 1, 1'-Binaphthyl

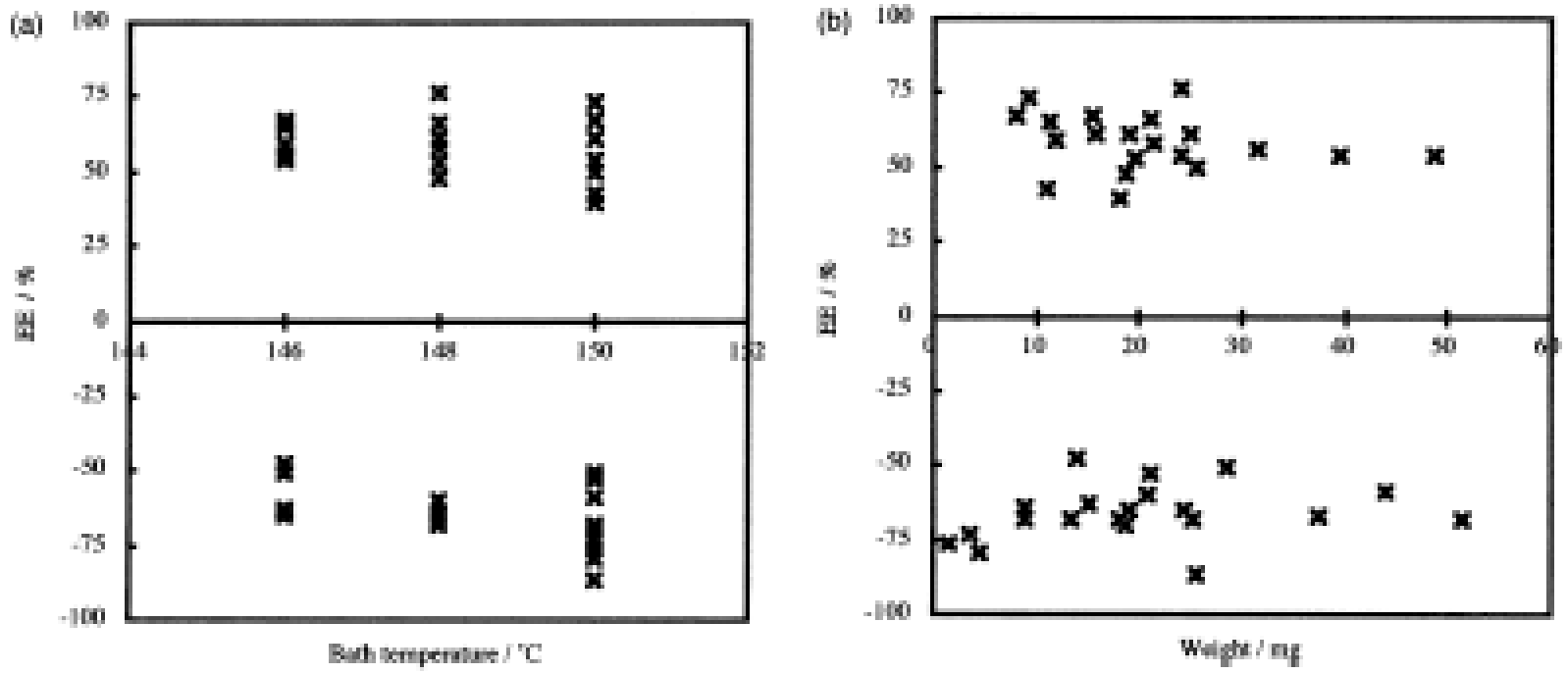

K. Asakura, D. K. Kondepudi, *et al.*, *J. Phys. Chem. B*, **2005**, *109*, 1586-1592.

Crystallization Front Model

Liquid phase: **L**

Growth layer: $\mathbf{G_S}$, $\mathbf{G_R}$

Interface of crystal to liquid: $\mathbf{I_S}$, $\mathbf{I_R}$

Crystal bulk phase: $\mathbf{C_S}$, $\mathbf{C_R}$

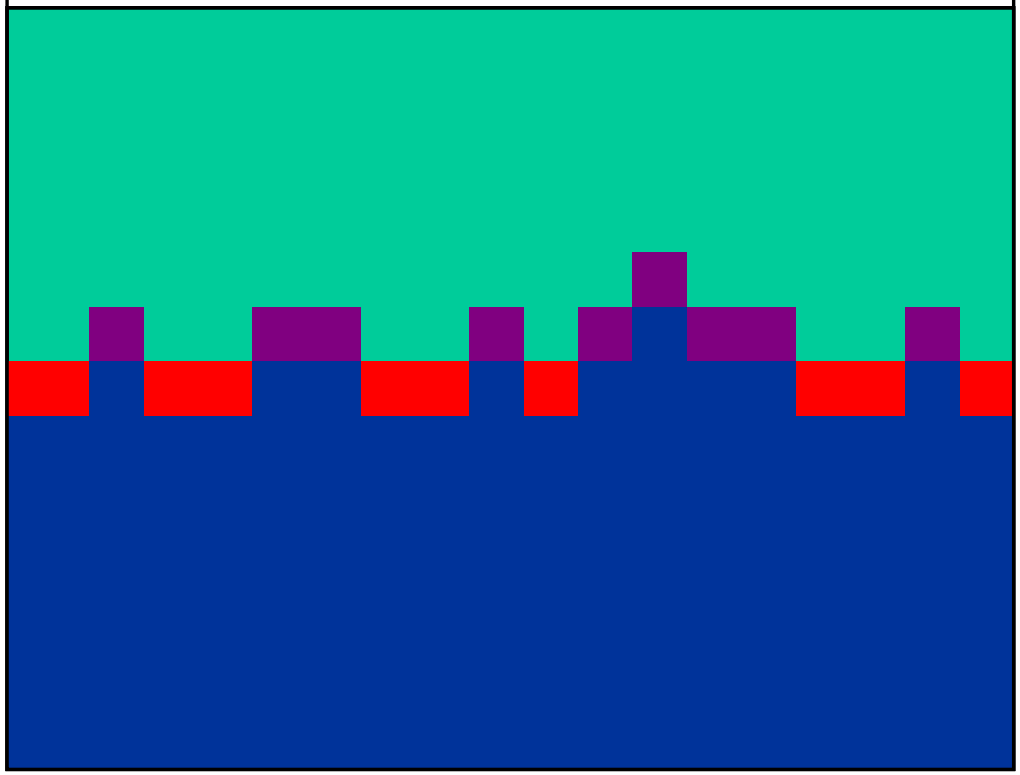

$$\mathbf{L} + \mathbf{I_S} \xrightarrow{k_{01}} \mathbf{G_S} + \mathbf{C_S}$$

$$\mathbf{L} + \mathbf{I_R} \xrightarrow{k_{01}} \mathbf{G_R} + \mathbf{C_R}$$

$$\mathbf{L} + \mathbf{I_S} \xrightarrow{k_{02}} \mathbf{G_R} + \mathbf{C_S}$$

$$\mathbf{L} + \mathbf{I_R} \xrightarrow{k_{02}} \mathbf{G_S} + \mathbf{C_R}$$

$$\mathbf{L} + \mathbf{I_S} + \mathbf{G_S} \xrightarrow{k_{11}} 2\,\mathbf{G_S} + \mathbf{C_S}$$

$$\mathbf{L} + \mathbf{I_R} + \mathbf{G_R} \xrightarrow{k_{11}} 2\,\mathbf{G_R} + \mathbf{C_R}$$

$$\mathbf{L} + \mathbf{I_S} + \mathbf{G_R} \xrightarrow{k_{12}} \mathbf{G_S} + \mathbf{G_R} + \mathbf{C_S}$$

$$\mathbf{L} + \mathbf{I_S} + \mathbf{G_R} \xrightarrow{k_{12}} 2\,\mathbf{G_R} + \mathbf{C_S}$$

$$\mathbf{L} + \mathbf{I_R} + \mathbf{G_S} \xrightarrow{k_{12}} 2\,\mathbf{G_S} + \mathbf{C_R}$$

$$\mathbf{L} + \mathbf{I_R} + \mathbf{G_S} \xrightarrow{k_{12}} \mathbf{G_S} + \mathbf{G_R} + \mathbf{C_R}$$

$$\mathbf{L} + \mathbf{I_S} + \mathbf{G_S} \xrightarrow{k_{13}} \mathbf{G_S} + \mathbf{G_R} + \mathbf{C_S}$$

$$\mathbf{L} + \mathbf{I_R} + \mathbf{G_R} \xrightarrow{k_{13}} \mathbf{G_S} + \mathbf{G_R} + \mathbf{C_R}$$

$$\mathbf{G_S} \xrightarrow{k_{20}} \mathbf{I_S}$$

$$\mathbf{G_R} \xrightarrow{k_{20}} \mathbf{I_R}$$

Kinetic Equations and Their Simplification

$$\frac{dG_S}{dt} = k_{01}I_S + k_{02}I_R + k_{11}I_SG_S + k_{12}\left(I_SG_R + I_RG_S\right) + k_{13}I_RG_R - k_{20}G_S$$

$$\frac{dG_R}{dt} = k_{01}I_R + k_{02}I_S + k_{11}I_RG_R + k_{12}\left(I_SG_R + I_RG_S\right) + k_{13}I_SG_S - k_{20}G_R$$

$$\frac{dI_S}{dt} = -k_{01}I_S - k_{02}I_S - k_{11}I_SG_S - 2k_{12}I_SG_R - k_{13}I_SG_S + k_{20}G_S$$

$$\frac{dI_R}{dt} = -k_{01}I_R - k_{02}I_R - k_{11}I_RG_R - 2k_{12}I_RG_S - k_{13}I_RG_R + k_{20}G_R$$

$$k_{02} \cong 0, k_{13} \cong 0$$

$$\frac{dG_S}{dt} = k_{01}I_S + k_{11}I_SG_S + k_{12}\left(I_SG_R + I_RG_S\right) - k_{20}G_S$$

$$\frac{dG_R}{dt} = k_{01}I_R + k_{11}I_RG_R + k_{12}\left(I_SG_R + I_RG_S\right) - k_{20}G_R$$

$$\frac{dI_S}{dt} = -k_{01}I_S - k_{11}I_SG_S + 2k_{12}I_SG_R + k_{20}G_S$$

$$\frac{dI_R}{dt} = -k_{01}I_R - k_{11}I_RG_R + 2k_{12}I_RG_S + k_{20}G_R$$

$$I_S + I_R + G_S + G_R = \text{Constant}(=1)$$

Steady State Solution of Kinetic Model

Symmetric steady state

$$\left[\begin{array}{l} G_S = G_R = \dfrac{-2k_{01}+k_{11}+2k_{12}-2k_{20}+\sqrt{(2k_{01}-k_{11}-2k_{12}+2k_{20})^2+4(2k_{11}+4k_{12})k_{01}}}{2(2k_{11}+4k_{12})} \\ I_S = I_R = \dfrac{2k_{01}+k_{11}+2k_{12}+2k_{20}-\sqrt{(2k_{01}-k_{11}-2k_{12}+2k_{20})^2+4(2k_{11}+4k_{12})k_{01}}}{2(2k_{11}+4k_{12})} \end{array}\right.$$

Asymmetric steady state

$$\left[\begin{array}{l} G_S = \dfrac{-k_{01}+k_{11}-k_{20}+\sqrt{(k_{01}-k_{11}+k_{20})^2+4k_{01}k_{11}}}{2k_{11}} \\ I_S = \dfrac{k_{01}+k_{11}+k_{20}-\sqrt{(k_{01}-k_{11}+k_{20})^2+4k_{01}k_{11}}}{2k_{11}} \\ G_R = I_R = 0 \end{array}\right.$$

$$\left[\begin{array}{l} G_S = I_S = 0 \\ G_R = \dfrac{-k_{01}+k_{11}-k_{20}+\sqrt{(k_{01}-k_{11}+k_{20})^2+4k_{01}k_{11}}}{2k_{11}} \\ I_R = \dfrac{k_{01}+k_{11}+k_{20}-\sqrt{(k_{01}-k_{11}+k_{20})^2+4k_{01}k_{11}}}{2k_{11}} \end{array}\right.$$

Back to Complex Kinetic Model

$$\frac{dG_S}{dt} = k_{01}I_S + k_{11}I_S G_S + k_{12}\left(I_S G_R + I_R G_S\right) - k_{20}G_S$$

$$\frac{dG_R}{dt} = k_{01}I_R + k_{11}I_R G_R + k_{12}\left(I_S G_R + I_R G_S\right) - k_{20}G_R$$

$$\frac{dI_S}{dt} = -k_{01}I_S - k_{11}I_S G_S + 2k_{12}I_S G_R + k_{20}G_S$$

$$\frac{dI_R}{dt} = -k_{01}I_R - k_{11}I_R G_R + 2k_{12}I_R G_S + k_{20}G_R$$

$$k_{02} \neq 0, k_{13} \neq 0$$

$$\frac{dG_S}{dt} = k_{01}I_S + k_{02}I_R + k_{11}I_S G_S + k_{12}\left(I_S G_R + I_R G_S\right) + k_{13}I_R G_R - k_{20}G_S$$

$$\frac{dG_R}{dt} = k_{01}I_R + k_{02}I_S + k_{11}I_R G_R + k_{12}\left(I_S G_R + I_R G_S\right) + k_{13}I_S G_S - k_{20}G_R$$

$$\frac{dI_S}{dt} = -k_{01}I_S - k_{02}I_S - k_{11}I_S G_S - 2k_{12}I_S G_R - k_{13}I_S G_S + k_{20}G_S$$

$$\frac{dI_R}{dt} = -k_{01}I_R - k_{02}I_R - k_{11}I_R G_R - 2k_{12}I_R G_S - k_{13}I_R G_R + k_{20}G_R$$

XRD Analysis of Crystal Phase of 1, 1’-Binaphthyl

1, 1’- XRD

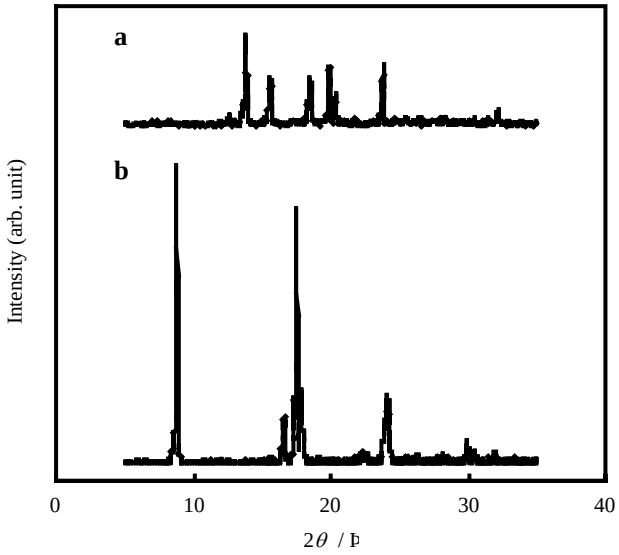

a: Chiral crystal

b: Racemic crystal

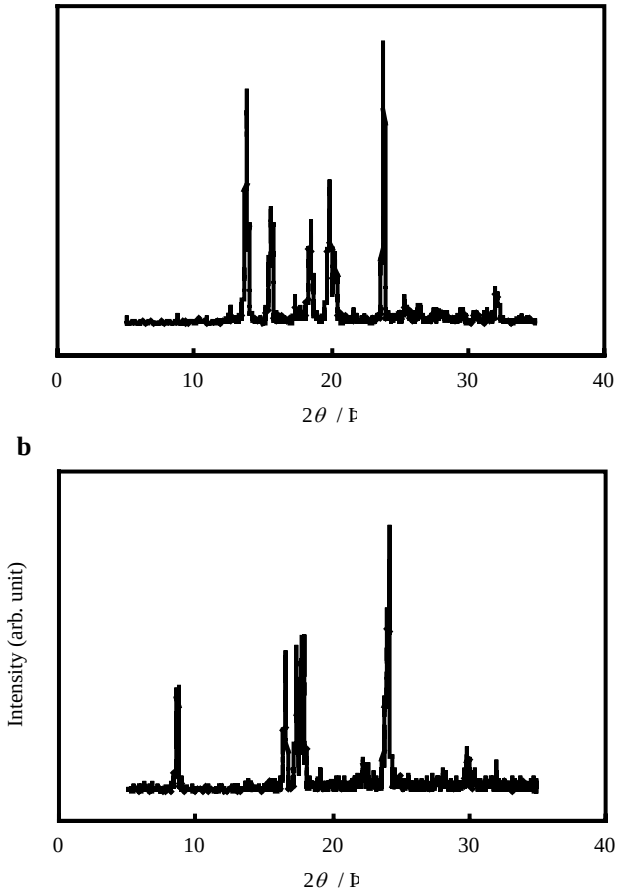

K. Asakura, D. K. Kondepudi, *et al.*, *Chirality*, **2004**, *16*, 131-136.

Linear Stability Analysis

Jacobian Matrix

$$\mathbf{J} = \begin{bmatrix} \frac{\partial(dG_S/dt)}{\partial G_S} & \frac{\partial(dG_S/dt)}{\partial G_R} & \frac{\partial(dG_S/dt)}{\partial I_S} & \frac{\partial(dG_S/dt)}{\partial I_R} \\ \frac{\partial(dG_R/dt)}{\partial G_S} & \frac{\partial(dG_R/dt)}{\partial G_R} & \frac{\partial(dG_R/dt)}{\partial I_S} & \frac{\partial(dG_R/dt)}{\partial I_R} \\ \frac{\partial(dI_S/dt)}{\partial G_S} & \frac{\partial(dI_S/dt)}{\partial G_R} & \frac{\partial(dI_S/dt)}{\partial I_S} & \frac{\partial(dI_S/dt)}{\partial I_R} \\ \frac{\partial(dI_R/dt)}{\partial G_S} & \frac{\partial(dI_R/dt)}{\partial G_R} & \frac{\partial(dI_R/dt)}{\partial I_S} & \frac{\partial(dI_R/dt)}{\partial I_R} \end{bmatrix}$$

$$= \begin{bmatrix} k_{11}I_S + k_{12}I_R - k_{20} & k_{12}I_S & k_{01} + k_{11}G_S + k_{12}G_R & k_{12}G_S \\ k_{12}I_R & k_{11}I_R + k_{12}I_S - k_{20} & k_{12}G_R & k_{01} + k_{11}G_R + k_{12}G_S \\ -k_{11}I_S + k_{20} & -2k_{12}I_S & -k_{01} - k_{11}G_S - 2k_{12}G_R & 0 \\ -2k_{12}I_R & -k_{11}I_R + k_{20} & 0 & -k_{01} - k_{11}G_R - 2k_{12}G_S \end{bmatrix}$$

Linear Stability Analysis

Eigenvalues for Asymmetric Solution

$$\lambda_1 = 0,\ \lambda_2 = -\sqrt{\left(k_{01} - k_{11} + k_{20}\right)^2 + 4k_{01}k_{11}}$$

$$k_{01} = 0.001,\ \ k_{12} = 0.002,\ \ k_{20} = 0.002,\ 0.005,\ 0.01$$

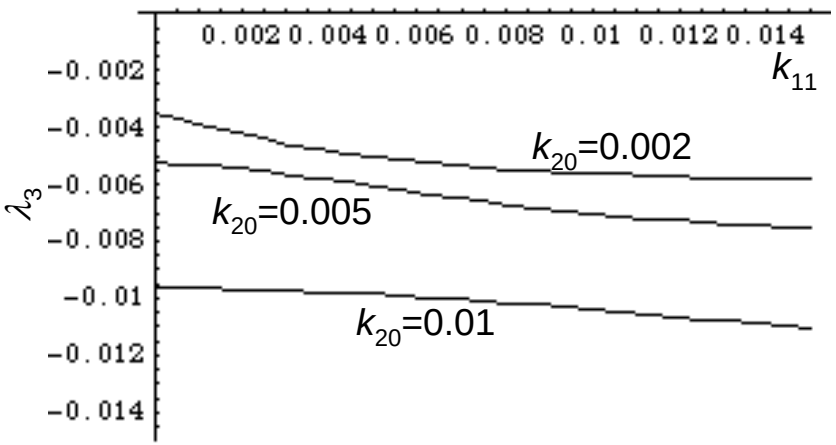

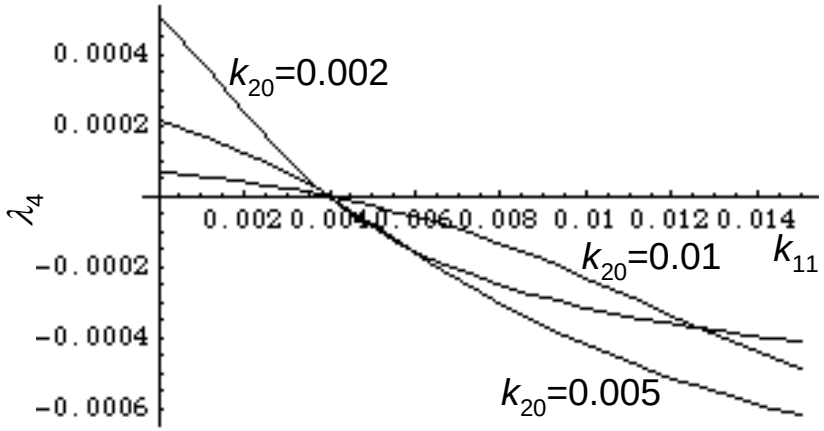

Linear Stability Analysis

Eigenvalues for Symmetric Solution

$$k_{01} = 0.001,\ \ k_{12} = 0.002,\ \ k_{20} = 0.002,\ 0.005,\ 0.01$$

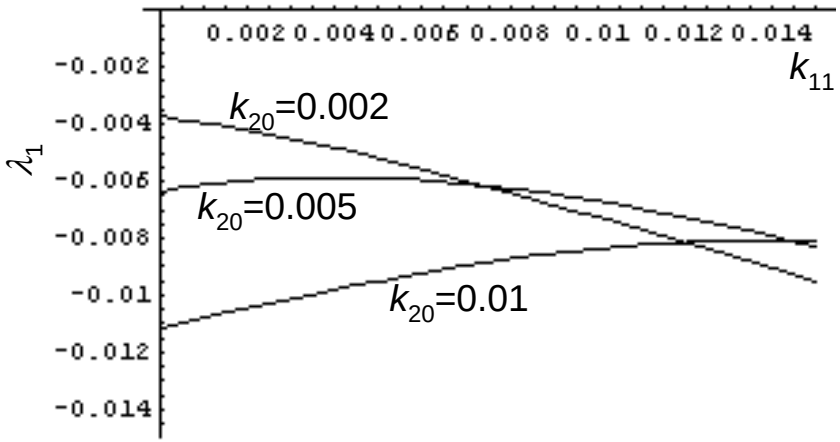

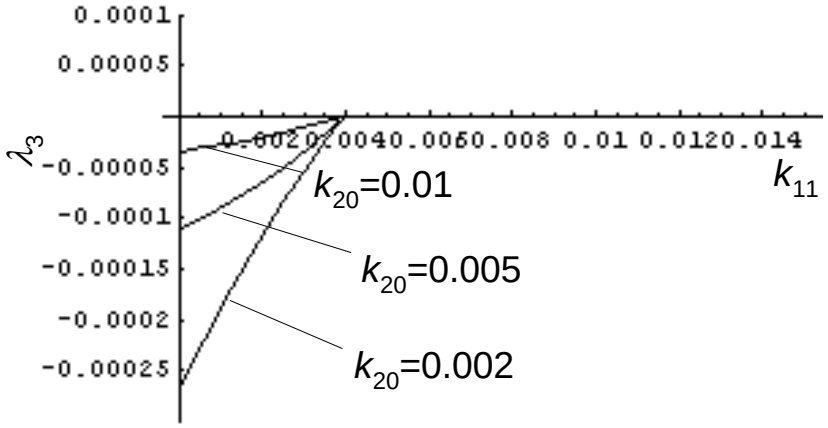

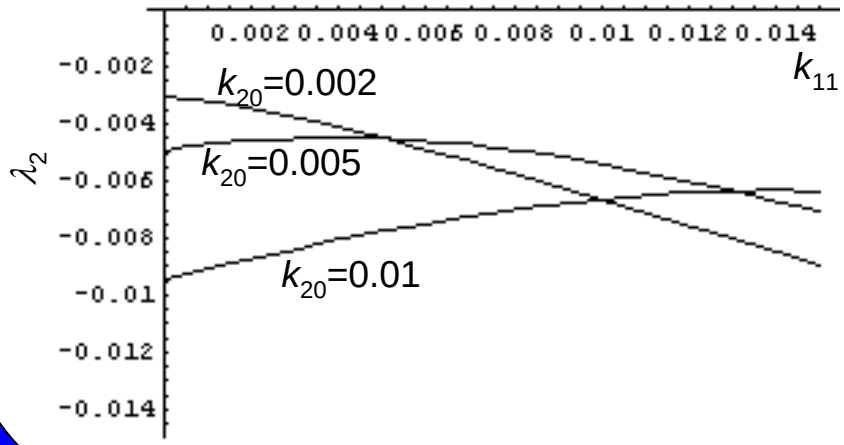

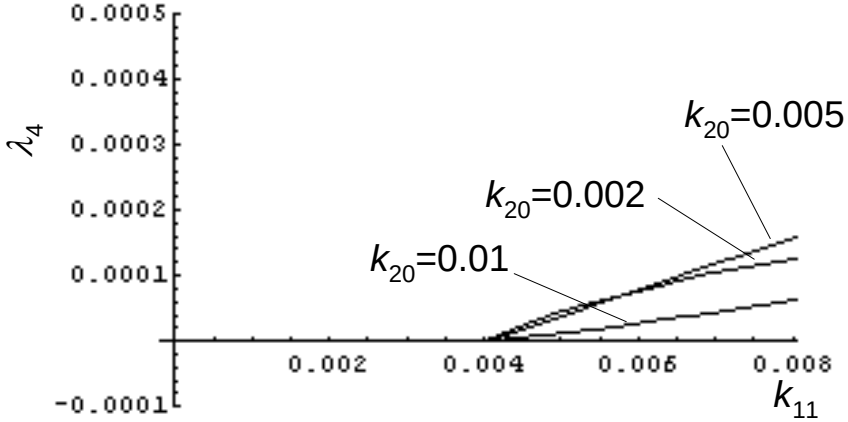

Bifurcation Diagram

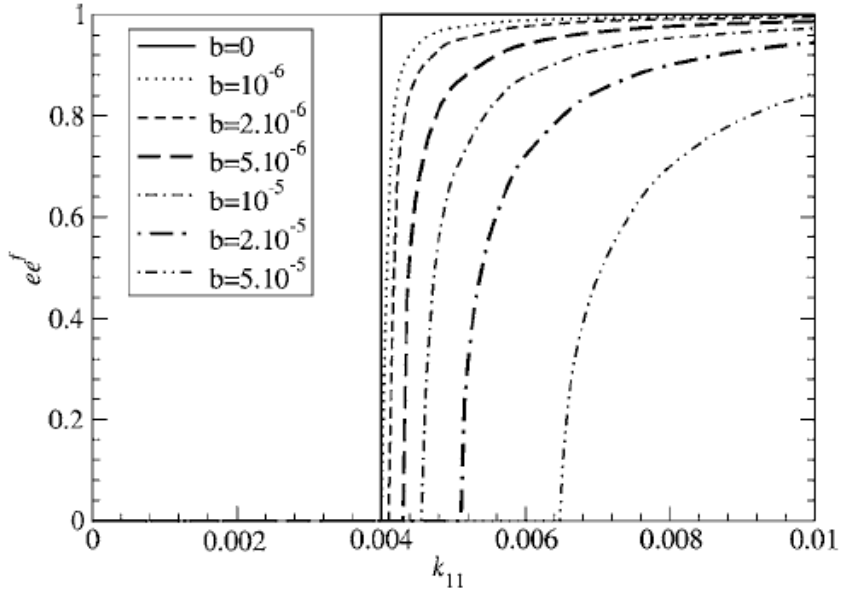

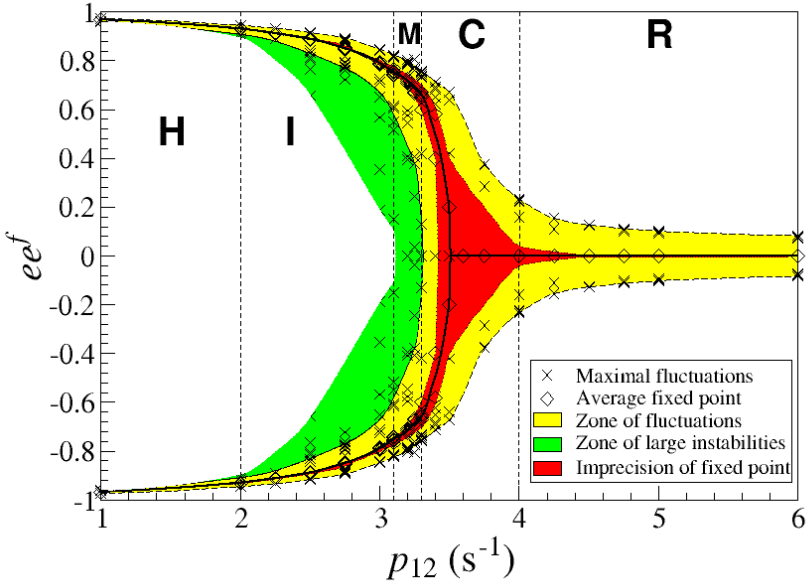

K. Asakura, R. Plasson,D. K. Kondepudi, *Chaos*, **2006**, *16*, 037116.

R. Plasson, D. K. Kondepudi, K. Asakura, *J. Phys. Chem. B*, **2006**, *110*, 8481-8487.

K. Asakura, D. K. Kondepudi, *et al.*, *J. Phys. Chem. B*, **2005**, *109*, 1586-1592.

Chiral Symmetry Breaking Transition

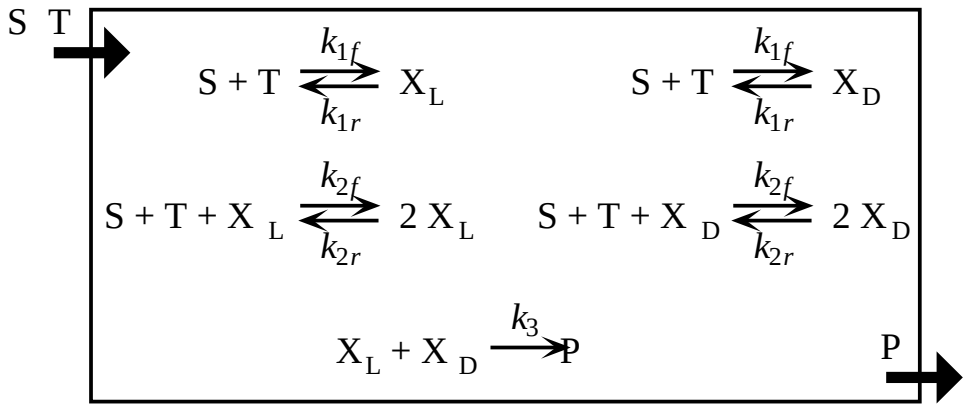

$$\lambda = [S][T]$$

$$\alpha = ([X_L] - [X_D]) / ([X_L] - [X_D])$$

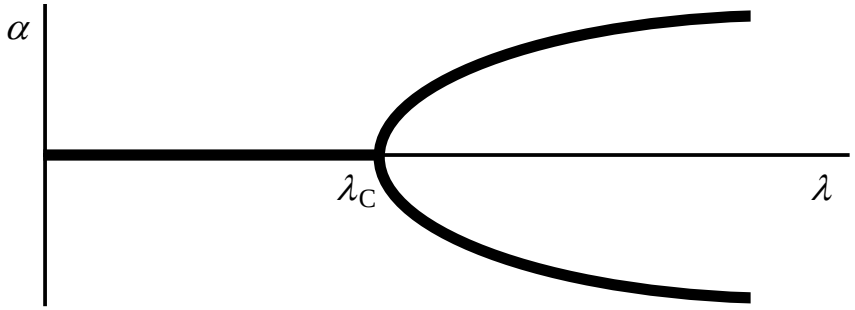

$$\frac{d\alpha}{dt} = -A\alpha^3 + B(\lambda - \lambda_C)\alpha$$

D. K. Kondepudi, G. W. Nelson, *Nature*, **1985**, *314*, 438-441.

Chirally Autocatalytic Reaction

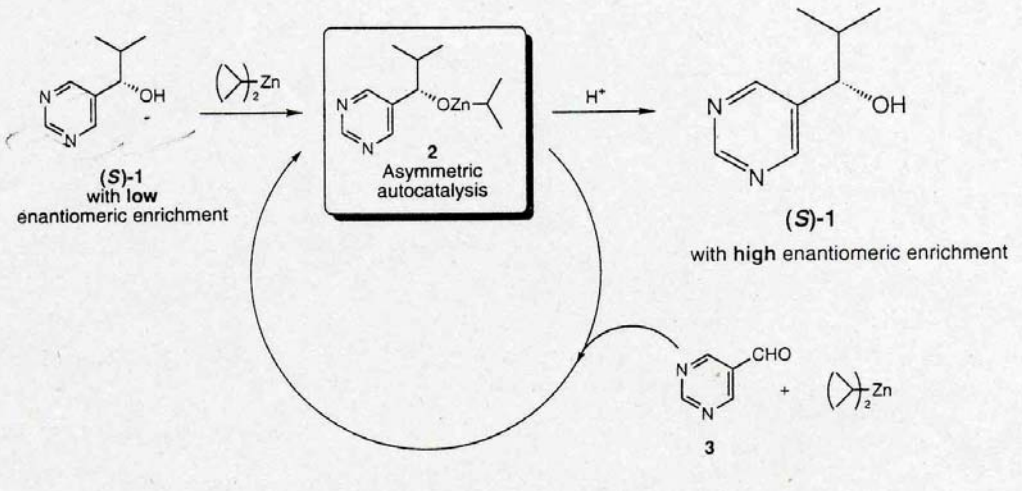

FIG. 2 Proposed reaction scheme of asymmetric autocatalysis of (*S*)-**1**.

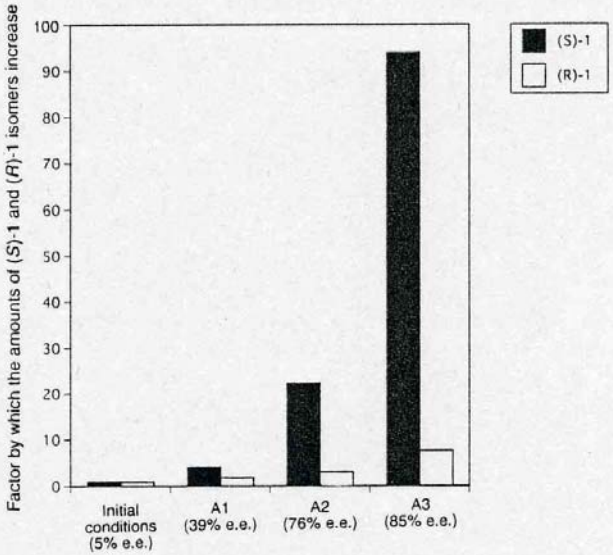

FIG 1. Asymmetric autocatalysis of chiral pyrimidyl alkanol (**1**). Runs A1–3 correspond to Table 1. The enantiomeric excess of (*S*)-**1** increases from 5 to 89% e.e. without the use of additional chiral auxiliaries. During the reactions (runs A1–3), the (*S*)-**1** increases by a factor of 94 times, while (*R*)-**1** increases by a factor of only eight times.

K. Soai, T. Shibata, H. Morioka, K. Choji, *Nature*, **1995**, *378*, 767-768.

Spontaneous Generation of Chiral Asymmetry by Soai Reaction

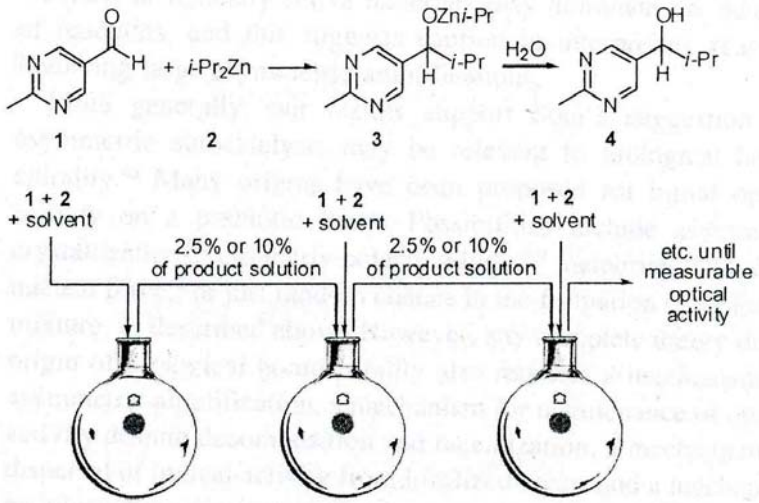

Figure 1. Process for replicative asymmetric amplification.

Table 1. Results from Trials of Replicative Asymmetric Amplification without Discrete Optically Active Additives

trial[a]	% ee[b]	trial[a]	% ee[b]	trial[a]	% ee[b]
1[c]	16 *S*[k]	17[g,i,u]	65 *S*[m]	33[e,s,u]	21 *S*[l]
2[c,t]	11 *S*[k], 78 *S*[l]	18[g,i,u]	70 *S*[m]	34[e,s,u]	81 *R*[l]
3[c,d]	18 *S*[k]	19[g,i,r,u]	85 *S*[l]	35[c,h,u]	29 *S*[l]
4[c,d]	16 *S*[k]	20[g,i,r,u]	86 *S*[l]	36[c,h,u]	29 *S*[l]
5[c,e,j]	32 *S*[l]	21[g,h,i]	48 *S*[l]	37[g,i,h,r,u]	18 *S*[l], 54 *S*[m]
6[c,f,j]	22 *S*[l]	22[g,h,i]	52 *S*[l]	38[g,i,u]	11 *S*[l], 42 *S*[n]
7[c,f,h,j]	30 *R*[m]	23[g,h,i,u]	48 *S*[l]	39[g,i,u]	5 *S*[k], 48 *S*[l]
8[c,e,h,j,t,u]	80 *S*[n]	24[g,i,u]	37 *S*[l]	40[g,i,u,v]	3 *S*[k], 43 *S*[l]
9[c,e,j,t,u]	75 *S*[n]	25[g,h,i]	32 *S*[l]	41[e,i,u]	18 *S*[m], 48 *S*[o]
10[c,h,u]	26 *R*[l]	26[s]	21 R[l]	42[e,i,u]	8 *S*[m], 32 *S*[n]
11[i,u]	54 *S*[l]	27[e,s]	67 *S*[m]	43[e,i,h,u]	4 *S*[p], 18 *S*[q]
12[c,h,u]	22 *R*[l]	28[e,j,s,u]	25 *R*[l]	44[e,i,u]	22 *S*[p], 45 *S*[q]
13[c,u]	23 *R*[l]	29[e,j,s,u]	32 *S*[l]	45[e,i,u]	5 *S*[m], 21 *S*[o]
14[c,h]	48 *R*[m]	30[e,j,s,u]	26 *R*[l]	46[e,i,u]	4 *S*[m], 24 *S*[o]
15[e,i]	21 *S*[m], 70 *S*[o]	31[e,j,s,u]	18 *S*[l]	47[e,h,i,u]	8 *S*[m], 26 *S*[o]
16[e,i]	13 *S*[l]	32[e,s,t]	34 *R*[l]	48[e,i,u]	13 *S*[m], 21 *S*[o]

[a] The trials employed the procedure of Figure 1, transferring 10% of the product solution at each generation unless otherwise noted. [b] Determined by NMR using $Eu(hfc)_3$. [c] Toluene solvent, reagent grade or purified as noted. [d] Solvent distilled from P_2O_5. [e] Solvent distilled from Na/benzophenone. [f] Solvent treated with H_2SO_4 followed by distillation. [g] Solvent purified by repeated crystallization. [h] New batch of solvent, relative to previous otherwise identical trials. [i] Benzene solvent, reagent grade or purified as noted. [j] Reaction in Teflon flask. [k] After second generation. [l] After third generation. [m] After fourth generation. [n] After fifth generation. [o] After sixth generation. [p] After seventh generation. [q] After eighth generation. [r] Transferring 2.5% of the product solution at each generation. [s] Ethyl ether solvent, reagent grade or purified as noted. [t] Reaction used a Teflon septum. [u] The pairs of trials 8/9, 12/13, 17/18, 19/20, 23/24, 28/29, 30/31, 33/34, 35/36, 37/38, 39/40, 41/42, 43/44, 45/46, and 47/48 were carried out side-by-side using identical reagents. [v] Absence of light.

D. A. Singleton, L. K. Vo,
J. Am. Chem. Soc, **2002**, *124*, 10010-10011.

Large Variation in ee and Rate of Reaction Observed in Soai Reaction

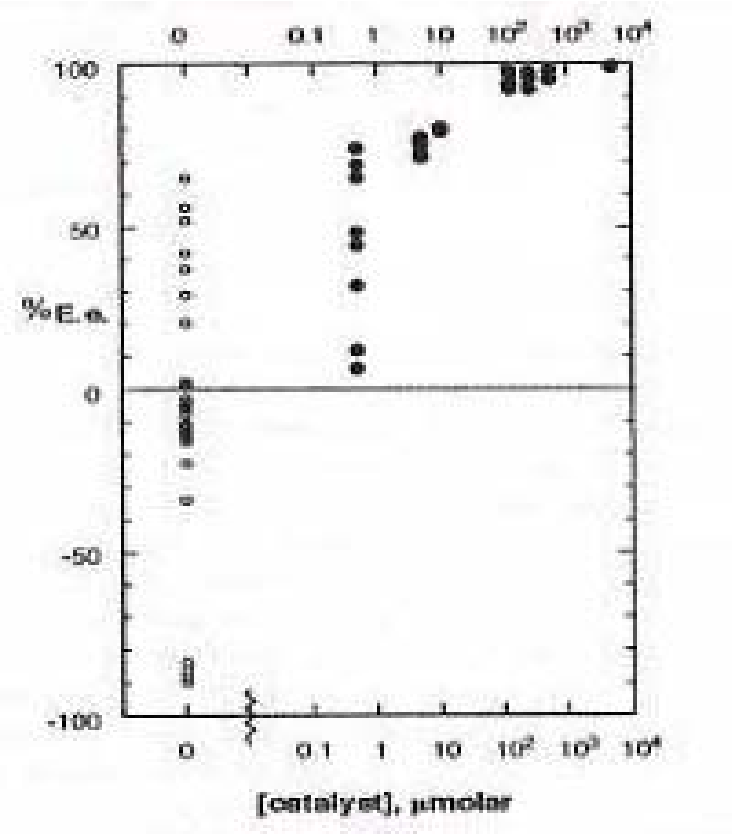

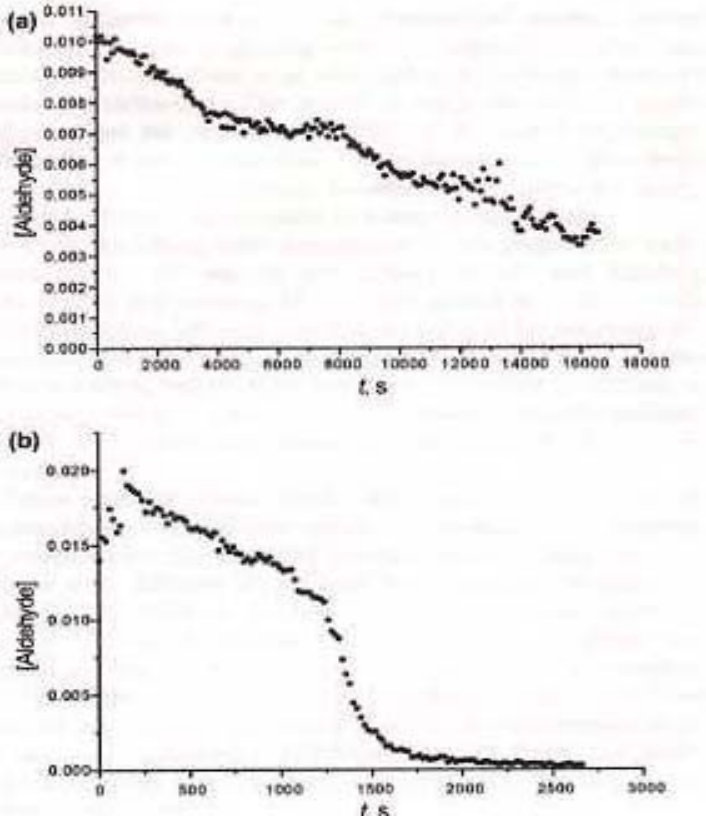

I. D. Gridnev, *Chem. Lett.*, **2006**, *35*, 148-153.

Crazy Clock

I. R. Epstein, *N ature*, **1995**, *374*, 321-327.

I. Nagypal, I. R. Epstein, *J. Chem. Phys.*, **1988**, *89*, 6925-6928.

$$4S_2O_3^{2-} + ClO_2^- + 2H_2O = 2S_4O_6^{2-} + 4OH^- + Cl^-$$

$$S_2O_3^{2-} + 2ClO_2^- + H_2O = 2SO_4^{2-} + 2Cl^- + 2H^+$$

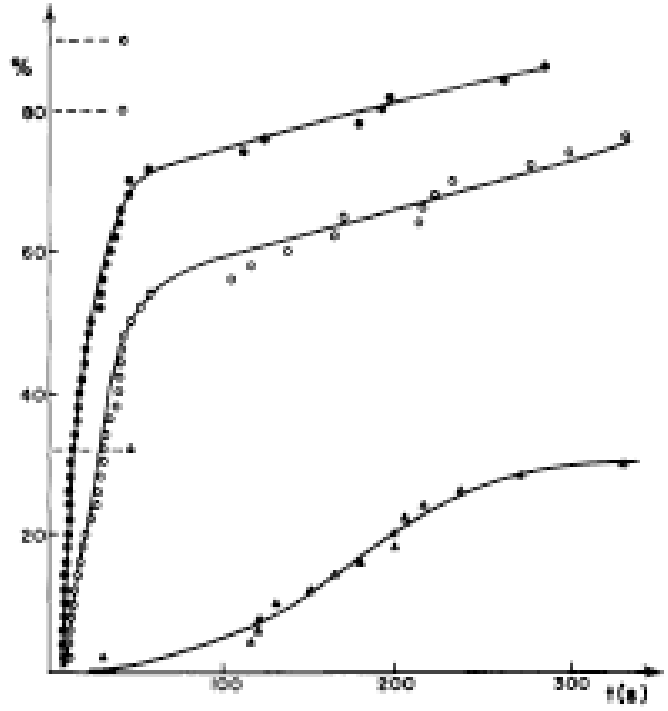

Figure 5. Cumulative probability distribution of reaction times at several stirring rates in a 4.00-cm^3 reaction mixture at 20.0 °C. Symbols: ●, 500 rpm; ○, 620 rpm; △, 760 rpm.

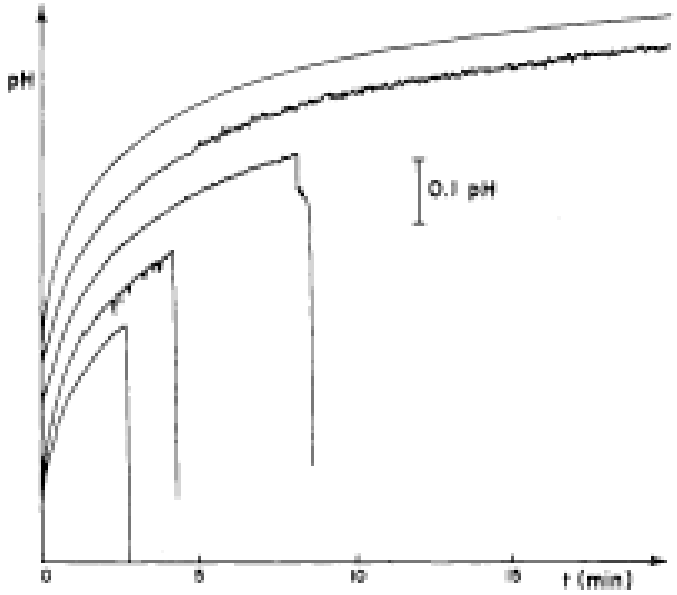

Figure 8. Representative pH traces of the reaction at 20.0 °C (see text). Successive curves are shifted by 0.07 pH units for better viewing, since in the absence of a shift, the initial portions of the curves coincide.